FRACTURE MECHANICS ANALYSIS OF NOVEL NON-RECTANGULAR STIFFENING CONCEPTS IN COMPARISON TO CONVENTIONALLY RECTANGULAR STIFFENED FUSELAGE STRUCTURES

S. Kébreau*
Institute of Aircraft Design and Lightweight Structures (IFL), Technical University of Braunschweig,
Hermann-Blenk-Straße 35, 38108 Braunschweig
GERMANY

ABSTRACT

This paper deals with the fracture mechanical analysis of metallic fuselage structures with non-rectangularly orientated stiffeners in comparison to a conventionally rectangular structure. Focus is on the analysis of the influence which the layout of different integrally stiffened structures has on the criticality of cracks. In this context different stiffening concepts were modelled and analysed with Finite Elements. Different crack scenarios were implemented and investigated under several static load cases in ANSYS with regard to the stress intensity factors at the crack tips based on linear fracture mechanics. A comparison presents the advantages and disadvantages of the different concepts.

NOTATION

A	Cross-sectional area	α	Cutout angle
E	Young's modulus	β	Tilt angle
F	Tensile force	ν	Poisson ratio
K	Stress intensity factor	σ	Tensile stress
V	Stiffener volume	τ	Shear stress
a	Half crack length	ρ	Density
b	Width	φ	Cylindric coordinate
l	Length		
p	Pressure		
r	Radius		

1. INTRODUCTION

In aircraft design, the fuselage structure is a significant parameter with regard to operating costs as well as manufacturing costs. Apart from efforts in the field of carbon reinforced plastics, aircraft designers are still interested in further development of metallic fuselage structures, as these structures allow e.g. the application of well established repair methods.

The usage of Aluminium-Lithium due to its welding and strength properties is one approach. Furthermore, a new approach within the development of metallic fuselage structures is the variation of the stiffening layout. In general, fuselage structures are stiffened in a rectangular way by stringers and frames. Due to new manufacturing methods, such as high speed cutting, other topologies are conceivable. However, a variation of the stiffening layout is expected to influence several properties, i.e. stability, producibility as well as fracture mechanical behaviour. The latter one is the objective of this paper.

2. ANALYSIS FLOW CHART

The flow chart in FIG. 2-1. provides an overview of the main steps which had to be performed for this analysis:

After defining the stiffening concepts, Finite Element models were built up in MSC PATRAN, including the crack implementation at defined locations and appropriate load cases. The models were solved and crack tip parameters were calculated in ANSYS.

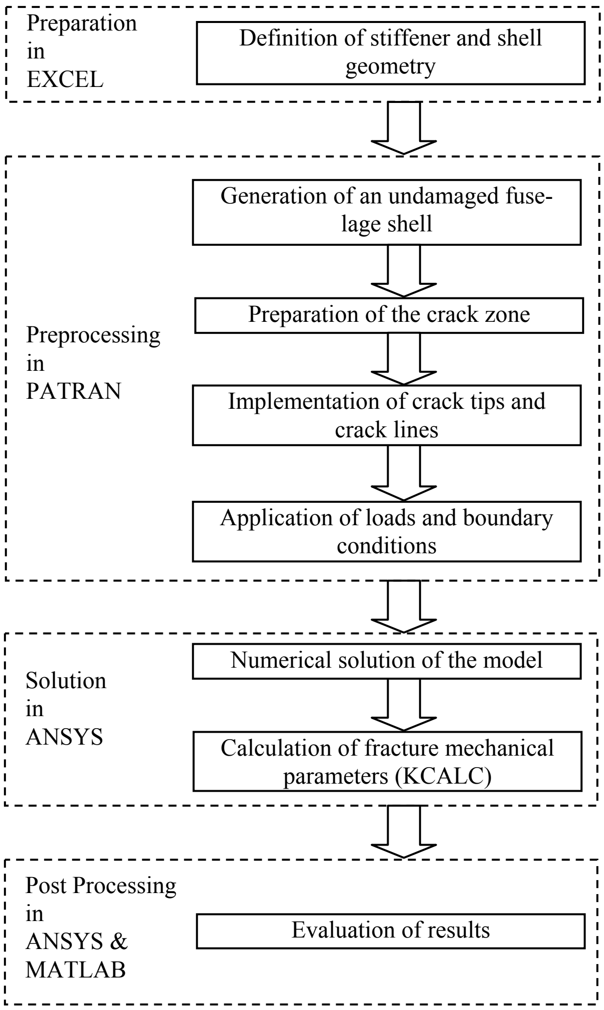

FIG. 2-1: Flow chart of the analysis

* Author contact from 01 / 2007 on: sebastian.kebreau@gmx.de / sebastian.kebreau@astrium.eads.net

3. CONCEPTS OF STIFFENING

The comparison in this paper deals with a conventionally rectangular stiffening concept as a reference concept and analyses two non-rectangular concepts. They are based on the requirement of mass constancy and are presented in the following sections. As a compromise between modelling expenditure and detail reproduction, a cutout segment of a fuselage is looked at (FIG. 3-1).

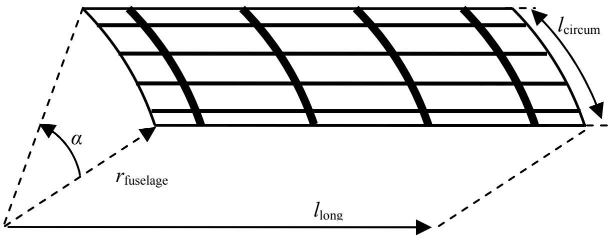

FIG. 3-1: Dimensions of a classical fuselage shell

It describes a length of l = 2134 mm and a cutout angle α = 14,4°. The fuselage radius amounts to r = 2820 mm. These dimensions correspond to the quad stringer and frame distance of an ordinary medium range airplane.

3.1. Conventionally rectangular structure "V1"

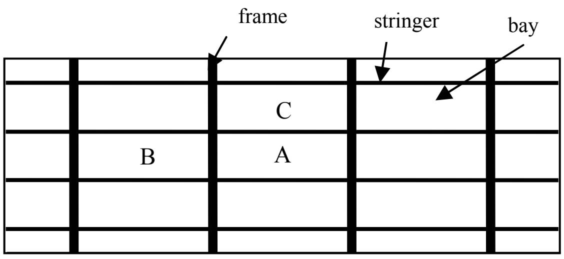

FIG. 3-2: Rectangular stiffening concept "V1"

Based on the indicated dimensions, the rectangular structure "V1" forms nine closed bays. This allows an examination of inner bay cracks as well as two bay cracks, without reaching the boundary region of the shell model. The stiffening components intersect at 90° in this concept (FIG. 3-2).

For a better comparability all concepts should be integrally stiffened. Since classical fuselages are differentially stiffened, the stiffener profiles were converted into integral producible double T profiles for these examinations. Highest priority was given to the constancy of mass compared to the differential version – which is effectively a constancy of cross-sectional area. Moreover, the geometrical moments of inertia should be of the same order. FIG. 3-3 and 3-4 show the stiffeners which result from an optimisation using a MICROSOFT EXCEL tool.

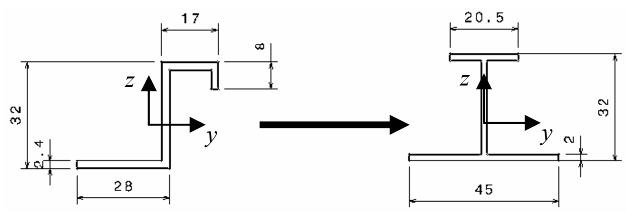

FIG. 3-3: Differential and integral stringer, concept "V1"

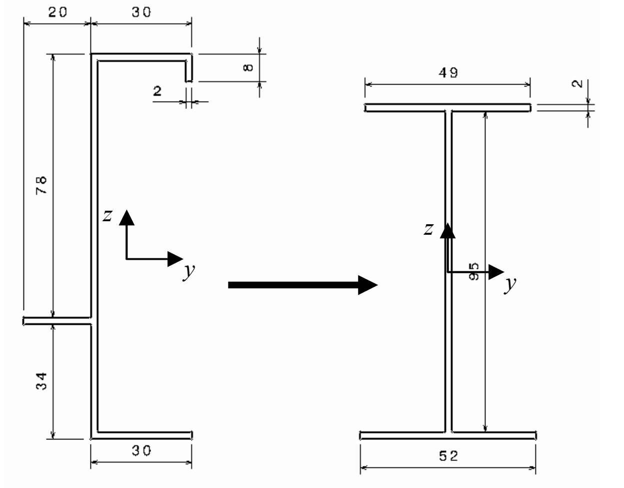

FIG. 3-4: Differential and integral frame, concept "V1"

3.2. Non-rectangular structure "V2"

Starting from the described rectangular stiffened reference structure, a non-rectangular stiffening concept was derived, preserving the mass of the fuselage shell. In concept "V2" the frames were retained while the stringers were replaced by tilted stiffeners, as indicated in FIG. 3-5.

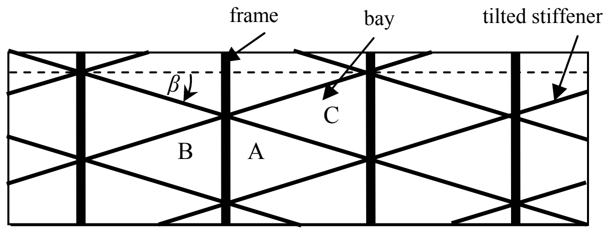

FIG. 3-5: Non-rectangular stiffening concept "V2"

The same mass of the fuselage structure was obtained by varying the tilted stiffeners. The geometrical interrelationship of the previous stringers and the tilted stiffeners can be derived from FIG. 3-5. Due to the tilt angle β = 18,372° the stiffeners become longer (scaled by 1/cos β), but must be less wide scaled by cos β to provide the same mass. This approach assumes that deviations in the intersection areas of tilted stiffeners and frames are negligible. The resulting geometry of one tilted stiffener of concept "V2" is presented in FIG. 3-6.

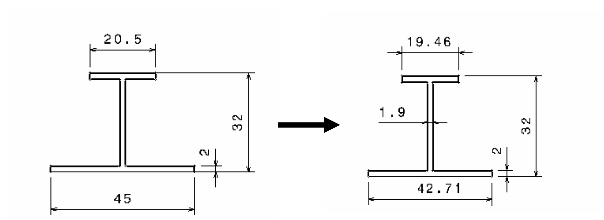

FIG. 3-6: Conversion of a stringer in concept "V1" into a tilted stiffener in "V2"

3.3. Non-rectangular structure "V3"

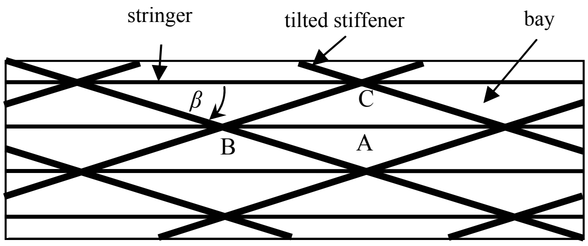

FIG. 3-7: Non-rectangular stiffening concept "V3"

The third stiffening concept (FIG. 3-7) contains longitudinal stiffeners comparable to the stringers of the reference concept "V1". However, instead of circumferential stiffeners this concept contains additionally tilted stiffeners. The circumferential loads, which are traditionally carried by frames, must be redistributed to these stiffeners.

Based on the requirement of mass constancy compared to the previous concepts, new profiles had to be defined. Due to the small tilt angle β, the tilted stiffeners have a high fraction of a longitudinal stiffening effect. Therefore, it was decided to reduce the longitudinal stiffeners' mass in favour of the tilted stiffeners. Since the skin of the shell remains unchanged, the total mass of the stiffeners in concept "V3" must be identical to the original total stiffener mass or volume of the reference structure "V1", assuming the same material density.

The stiffener volume of "V1" is:

$$(1)\quad V_{\mathrm{stiff,V1}} = 4\cdot A_{\mathrm{str,V1}}\cdot l_{\mathrm{long}} + 4\cdot A_{\mathrm{frame}}\cdot l_{\mathrm{circum}} \approx 2700000\ \mathrm{mm}^3$$

Neglecting deviations from the intersection regions of tilted stiffeners and stringers, the volume of the stiffeners in "V3" follows from:

$$(2)\quad V_{\mathrm{stiff,V3}} = 4\cdot A_{\mathrm{tilted,V3}}\cdot \frac{l_{\mathrm{long}}}{\cos\beta} + 4\cdot A_{\mathrm{str,V3}}\cdot l_{\mathrm{long}} \overset{!}{=} V_{\mathrm{stiff,V1}}$$

According to the previous considerations to reduce the longitudinal stiffener volume, the following profile geometries were defined:

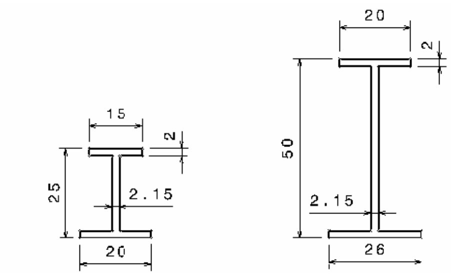

FIG. 3-8: Stiffener profiles of stringer (left) and tilted stiffener (right) in concept "V3"

4. FINITE ELEMENT MODEL

This section presents the generation of the Finite Element model and the corresponding boundary conditions.

4.1. Uncracked structure generation

The model generation of a fuselage section shell with one of the stiffening concepts "V1", "V2" or "V3" was performed in parametric PATRAN Command Language (PCL) routines that enabled a shell generation based on few parameters such as fuselage radius, cutout angle of the shell as well as frame distance, height and width of the stiffeners. The routines generated the curves and surfaces which were necessary for the following Finite Element mesh generation. This includes in particular the generation of the complex intersection areas, which result from the intersection of two tilted stiffeners and a frame or a stringer, respectively.

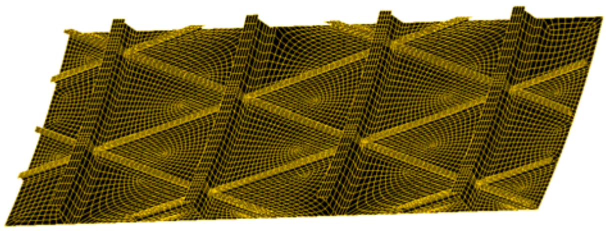

FIG. 4-1: FE-mesh of an uncracked shell "V2"

The resulting model was meshed with 4-node-shell elements with an order of magnitude of "10 mm". This mesh resolution yields approximately a number of 18000 elements. Their properties were chosen according to the material data mentioned in section 4.4.. FIG. 4-1 depicts exemplarily the mesh of a "V2" shell.

4.2. Crack scenarios

Cracks can appear at various locations in a fuselage structure. For the assessment of the different stiffening concepts crack scenarios for an appropriate comparison had to be chosen. In the present analyses, crack scenarios are limited to those within the skin. The growth within the stiffeners is not considered, as this depends on the stiffener profile geometry itself.

For a manageable comparison, the reduction to a few crack locations and orientations was necessary (FIG. 4-2).

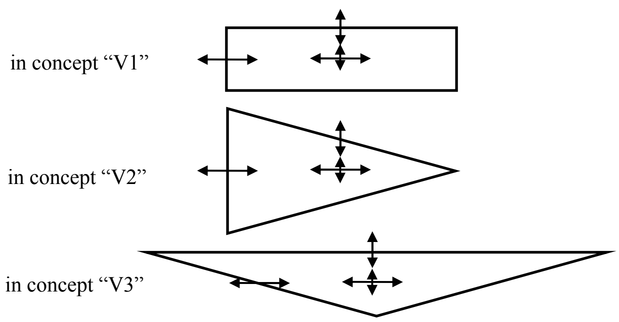

FIG. 4-2: Schematic layout of crack scenarios inside one bay and exceeding the limiting stiffener (two bay crack)

Longitudinal and circumferential cracks are analysed both for one bay cracks (not exceeding any stiffener) and two bay cracks, where the two crack tips are located in two adjoining bays. The centres of the cracks are located at the half height and half width of each bay for reasons of comparability. The crack length was varied from this starting point. The chosen bays are central bays (indicated as "A" in FIG. 3.2, 3.5 and 3.7), to reduce the effects of boundary conditions. The two bay cracks start with an already broken stiffener and were modelled into the bays “A” & “B” for longitudinal cracks or “A” & “C” for circumferential cracks. The assumption of a uniform crack growth at both crack tips is idealised, but provides a better comparability with the other concepts.

4.3. Crack implementation

The Finite Element model (FIG. 4.1) was generated without any cracks, as the needs of the crack tips are different with regard to the elements in this local region. The previously generated shell elements are not applicable to an analysis of the crack tip reaction.
As the stresses increase with $r^{-(1/2)}$ in linear elastic theory when approaching the crack tip, this singular behaviour had to be treated separately. Variable r is the radial distance from the crack tip. A crack tip element has to be of a higher order than the generally used 4-node-shell-elements and the position of the middle node has to be at one quarter of the element’s edge length [1], as indicated by the nodes “V”, “X”, “R” and “T” of the prism elements in FIG. 4-3. These three dimensional SOLID95-elements [2], consisting of 20 nodes, were applied to obtain three dimensional crack tip results in ANSYS.

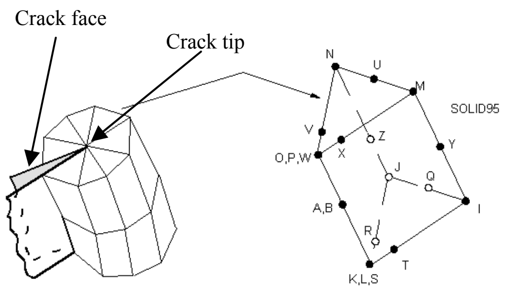

FIG. 4-3: SOLID95-elements with a middle node on the quarter position for modelling a crack tip singularity [2]

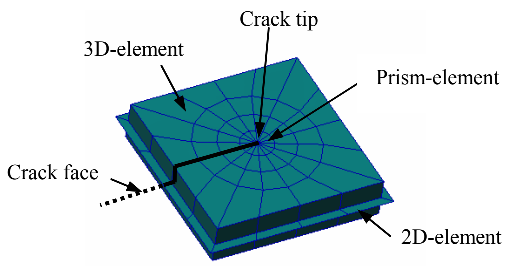

FIG. 4-4: Crack tip square consisting of 3D- and 2D-elements

The modelling guidelines were implemented into a PCL routine to generate crack tips at two defined locations and a crack face between these tips. The closest zone around the tip consists of 3D-elements. They pass into a region of 2D-elements which allow the connection to the remaining existing 2D-elements of the fuselage shell. For connecting the crack tip square (shown in FIG. 4-4) to the remaining structure, the generation of several surfaces was necessary because it must be guaranteed that nodes at the crack face are not connected.
Since the element size of the crack tip square is considerably smaller than the elements of the remaining model, a smooth transition had to be performed. Based on the “One Way Bias” option for non-linear mesh seed and the “Paver” method for the mesh generation a crack implementation routine was realised in MSC PATRAN.
FIG. 4-5 gives an example of the implementation of the two crack tip squares into the triangular bay of concept “V2”. The positions of the crack tips were defined parametrically to enable a variation of crack lengths.

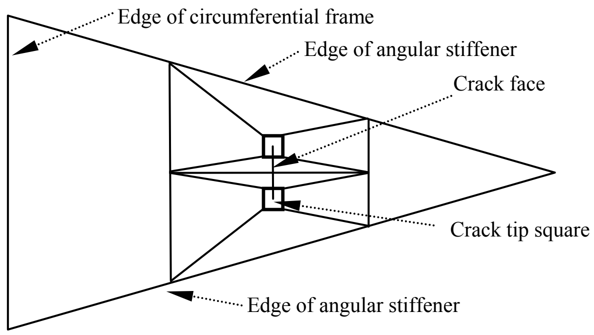

FIG. 4-5: Crack tips and crack face in the context of a triangular bay in “V2”

4.4. Material selection

Since the considered structures are integral ones, the material properties of the higher-tensile and weldable Aluminium-Lithium alloy were chosen ($E = 76000$ MPa). Different properties, applied to all models, would yield different results from an absolute point of view, but not affect the comparison between the concepts since the linear stress intensity calculation results from the displacements within the crack tip (cf. section 5.1).

4.5. Load cases and boundary conditions

For the crack analysis, a suitable load is mandatory to stress the crack tip in a way which would cause a crack growth. Since the stresses in the cracked bay are not known due to the stiffening effects, at least the global loads are orientated perpendicularly to the crack orientation.

4.5.1. Longitudinal cracks

The load case for longitudinal cracks is a combination of internal pressure, tensile force and a displacement set. As internal pressure in a cylinder causes hoop stresses, the model, which is effectively a cutout α of a cylinder, was loaded by a tensile force F on the upper and lower edge and a pressure p, which acts on the surface. The necessary tensile load is a result of the equilibrium of forces, which can be reduced from

(3) $$p \cdot A_{\text{proj}} \cdot \cos\left(\frac{\alpha}{2}\right) = F \cdot \cos(90° - \alpha)$$

to

(4) $$F = p \cdot b \cdot r$$

by algebraic manipulation, where the force is dependant from the pressure, the cylinder radius and the width b, which is the out-of-plane direction in FIG. 4-6.

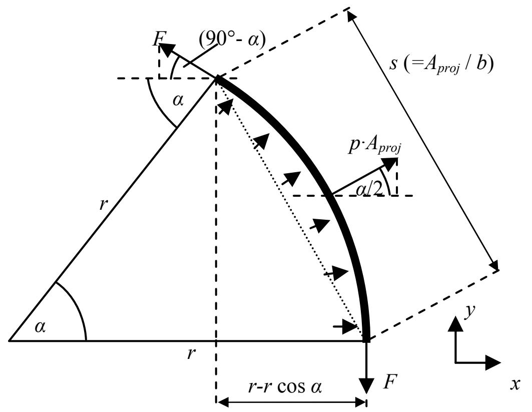

FIG. 4-6: Geometrical dependencies and loads in equilibrium

The pressure was defined as

(5) $$p = 2 \cdot \Delta p_{\text{operational}} = 2 \cdot 0{,}0593 \frac{\text{N}}{\text{mm}^2} = 0{,}1186 \text{MPa}$$

for an orientation towards a typical value. This corresponds to a force

(6) $$F = 0{,}1186 \cdot 533{,}5 \cdot 4 \cdot 2820 \text{ N} \approx 713720 \text{ N}$$

Additionally to the impressed loads, displacements were defined. The rotational degrees of freedom were locked to take the moments especially in the cut tilted stiffeners. The radial displacements of the four edges were also locked for a better reproduction of the circular global shell shape.
For a uniform load application, the tangential displacements of the upper edge nodes were coupled with "Multi Point Constraints" (MPC) so that the load F applied on one node, was uniformly distributed to all nodes of the edge. The nodes of the lower edge were also coupled by MPC and locked into tangential direction to provide a bearing of the model.

4.5.2. Circumferential cracks

Circumferential cracks were stressed by a load in longitudinal direction of the shell. The tensile load was applied to the side edges of the shell. The upper and the lower edges were coupled regarding the displacements and rotations to approximate the cylindrical character. This coupling was performed using a routine that identifies the opposing nodes of the edges. The lateral edges, to which the load was applied, were not coupled since the influence on the crack was expected to be small due to the longish shape of the shell. For keeping the order of magnitude, the force was determined from the pressure p pressing on an imaginary cylinder cover:

(7) $$\begin{aligned} F &= \pi \cdot r^2 p \cdot \frac{\alpha}{360°} \\ &= \pi \cdot 2820^2 \text{mm}^2 \cdot 0{,}1186 \frac{\text{N}}{\text{mm}^2} \cdot \frac{14{,}4°}{360°} \approx 118500 \text{ N} \end{aligned}$$

Similar to the previous load case, the force was applied uniformly to all nodes of the lateral edges.

4.5.3. Shear-tension

A further group of load is a shear-tension combination, which appears depending on the position in the fuselage. A complete coupling of the opposing nodes on the upper and lower edge was carried out. Additionally, the lateral edges were coupled regarding the rotational degrees and the radial displacement. The bearing was realised by locking the axial and circumferential displacement on the left edge. The application of shear and tensile forces was performed on the right edge. The tensile forces were applied to the whole edge, while shear stress was applied to the cut edge of the skin. This is based on the assumption that shear stress is mainly transmitted by the skin. The loads were chosen to the extent that the shear stress yields $\tau = 150$ MPa. The tensile force was varied to get different shear-tensile-ratios of $\tau / \sigma = 0{,}75 \ldots 4$.

5. RESULTS

Before the discussion of the results of the numerical analysis, theoretical basics and definitions concerning the stress intensity factor and crack deflection are given.

5.1. Stress intensity factor *K*

One meaningful parameter for the fracture mechanical characterisation of the crack tip in linear theory is the stress intensity factor. The behaviour of a stressed crack tip can be divided into three modes, shown in FIG. 5-1.
Mode I describes a crack opening due to a load perpendicular to the crack surface. Mode II is a sliding of the opposing crack surfaces within the plane, whereas Mode III is an out-of-plane shear displacement. In all modes, the stresses are a function of the angle φ and increase with $r^{-(1/2)}$ where r is the distance from the crack tip (FIG. 5-2). The stress does not only depend on the location referred to the crack tip, but also on the stress intensity factor.

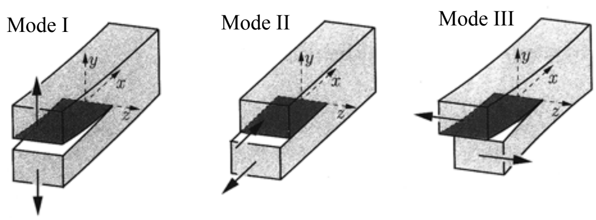

FIG. 5-1: Three failure modes of a crack tip [3]

(8) Mode I: $$\begin{Bmatrix} \sigma_x \\ \sigma_y \\ \tau_{xy} \end{Bmatrix} = \frac{K_I}{\sqrt{r}} \begin{pmatrix} f_1(\varphi) \\ f_2(\varphi) \\ f_3(\varphi) \end{pmatrix}$$

(9) Mode II: $$\begin{Bmatrix} \sigma_x \\ \sigma_y \\ \tau_{xy} \end{Bmatrix} = \frac{K_{II}}{\sqrt{r}} \begin{pmatrix} f_4(\varphi) \\ f_5(\varphi) \\ f_6(\varphi) \end{pmatrix}$$

(10) Mode III: $$\begin{Bmatrix} \tau_{xz} \\ \tau_{yz} \end{Bmatrix} = \frac{K_{III}}{\sqrt{r}} \begin{pmatrix} f_7(\varphi) \\ f_8(\varphi) \end{pmatrix}$$

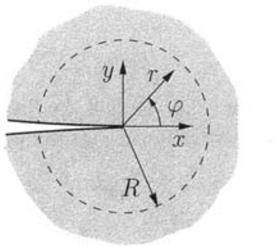

FIG. 5-2: Crack tip in polar coordinates [3]

This is an amplification factor which is dependant on the geometry and the applied load. Thus, the factor is a suitable factor to quantify the influence of the stiffening concept on the crack tip criticality. The higher the stress intensity factor the higher the crack tip load will be. According to Hooke's law, the expressions (8…10) can be transformed into equations of the form

$$K_i = f(r, \Delta u_i) \tag{11}$$

where Δu_i is the displacement (in y for K_I, in x for K_{II} and out-of-plane for K_{III}) of a defined location close to the crack tip. In this way, a calculation of the stress intensity factor is performed from the displacement results in ANSYS. A special function "KCALC" in ANSYS enables this calculation from the nodes within the crack tip elements (FIG. 4-3).

5.2. Crack deflection

In case of mixed fracture modes, a crack deflection arises. Different theories for the prediction exist. One well-known criterion is the criterion of maximal hoop stress, presented by *Erdogan* and *Sih* [7]. It is expected, that the crack will grow into the direction which maximises the hoop stress. This results in the following crack propagation angle, which will also be considered in selected cases.

$$\varphi_0 = -\arccos\left[\frac{3\cdot\left(\frac{K_{II}}{K_I}\right)^2 + \sqrt{1+8\cdot\left(\frac{K_{II}}{K_I}\right)^2}}{1+9\cdot\left(\frac{K_{II}}{K_I}\right)^2}\right] \tag{12}$$

5.3. Discussion of stress intensity factors

The judgement of the stiffening concepts is carried out based on the stress intensity factor as a function of the crack length. This allows the valuation of the criticality at the crack tip. The results of the traditional concept "V1" are taken as a reference to compare the non-rectangular concepts to it.

5.3.1. Central longitudinal one bay crack

For the central longitudinal one bay crack, it is assumed that the crack develops uniformly into both directions. The stress plots in FIG. 5-3 depict the circumferential stresses in the bays of concepts "V1", "V2" and "V3". For reasons of Finite Element modelling, cracks could only be modelled to a length of 93 %, 80 % and 84 % respectively of the bay width. The cracks do consequently not reach the stiffeners. The displacements indicated in the crack region are scaled up to demonstrate the crack opening. The stress fields show the typical stress free zone at the crack faces and the obvious stress concentration at the crack tips. The protecting effect of the triangle in "V2" where the stress is significantly lower and the extended zone of higher stress in "V3" are conspicuous. Slight stress asymmetries between the crack tip sides in "V3" are due to the fact that the examined bay is not located symmetrically on the shell. The following curve (FIG. 5-4) shows the crack tip stress intensity of Mode I for the different stiffening concepts. For reasons of information redundancy, only one side is evaluated for versions "V1" and "V3" while concept "V2" provides different information on both crack tip sides.

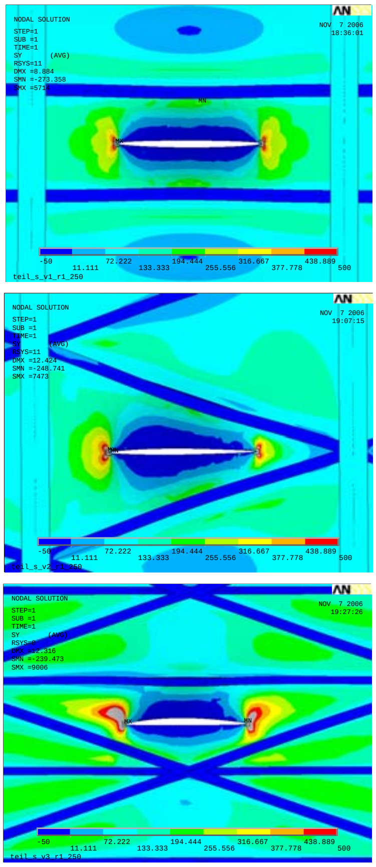

FIG. 5-3: Circumferential stresses for longitudinal one bay cracks, concepts "V1", "V2" and "V3"

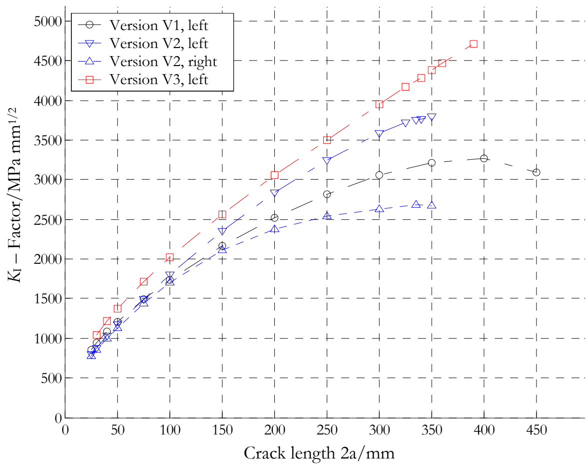

FIG. 5-4: K_I-Factor in a central one bay crack, stiffening concepts "V1", "V2" and "V3"

Considering the left crack tip, K_I yields 937 MPa mm$^{(1/2)}$ for a small crack of 2a = 30 mm. Concept "V2" yields a slightly lower stress intensity of 879 MPa mm$^{(1/2)}$ while the severest crack tip situation is found for concept "V3", K_I = 1047 MPa mm$^{(1/2)}$, as "V3" has the weakest circumferential stiffening. "V2" has additional circumferential stiffening effects from the angular stiffener. With increasing crack length, an increase in crack tip intensity can be qualitatively noticed for all concepts. However, the gradients differ considerably.

Highest K_I are found in “V3”, where the stress intensity increases nearly linearly: The approaching tilted stiffeners have no remarkable protecting influence on the crack tip, since the inclination is small. “V2” is influenced by two superimposing effects: A crack prolongation on the left side brings the crack tip closer to the circumferential stiffener, but the tilted stiffeners’ distance increases. This leads to a moderate increase compared to “V3”, but still worse than in “V1”. The left crack tip of the conventional “V1” has the lowest increase. A maximum is reached definitely before the stiffeners are reached. Beyond a crack length of $2a$ = 400 mm a further crack growth reduces the criticality of the crack tip, as indicated by the negative gradient dK/da. Contrary to “V1” and “V3”, the right crack tip of “V2” provides additional information: As the crack grows into the triangular edge of the bay, the K_I -Factor develops less critically and is below the curve of “V1”. After a crack length of 300 mm, there is hardly further increase since progressive stiffening compensates for additional crack length effects.

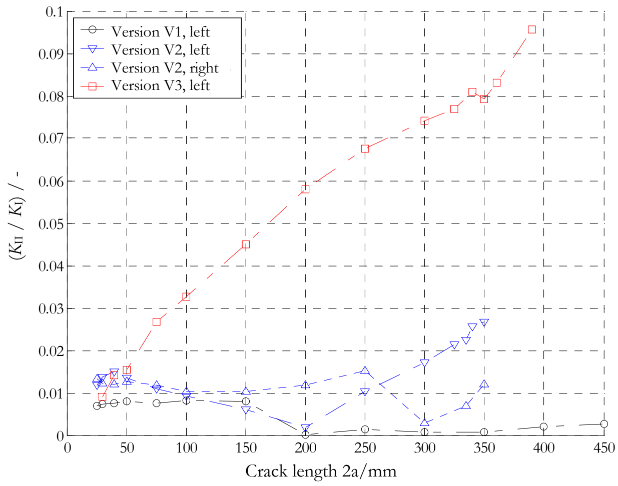

FIG. 5-5: Ratio of K_{II} / K_I in a central longitudinal one bay crack

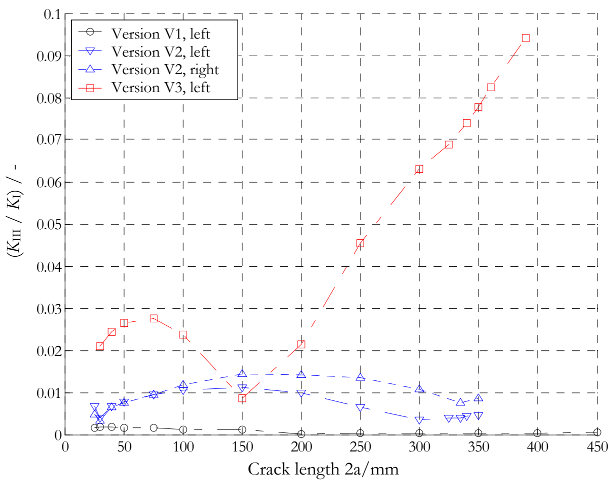

FIG. 5-6: Ratio of K_{III} / K_I in a central longitudinal one bay crack

Although the global loads were chosen to stress the crack mainly in Mode I, the other modes are evaluated, too. They can appear due to the stiffening effects or as a result of a pressurised damaged bay. FIG. 5-5 and 5-6 show the crack tip intensities K_{II} and K_{III} referred to the main mode K_I: Modes II and III are practically absent in concept “V1”, they are below 1 % of the stress intensity of Mode I. Concept “V2” has also a very low ratio of less than 3%. In “V3” however, they appear with almost 10 %. The shear effect within the crack tips (Mode II) can be explained by unsymmetrical stiffening of the upper and lower part of the bay. Different Mode III stress intensities are due to the “bulging” effect, which can often be noticed within pressurised asymmetrical structures [9]. Thus, concept “V3”, which is already highly stressed in Mode I, is additionally stressed in the other modes.

5.3.2. Central longitudinal two bay crack

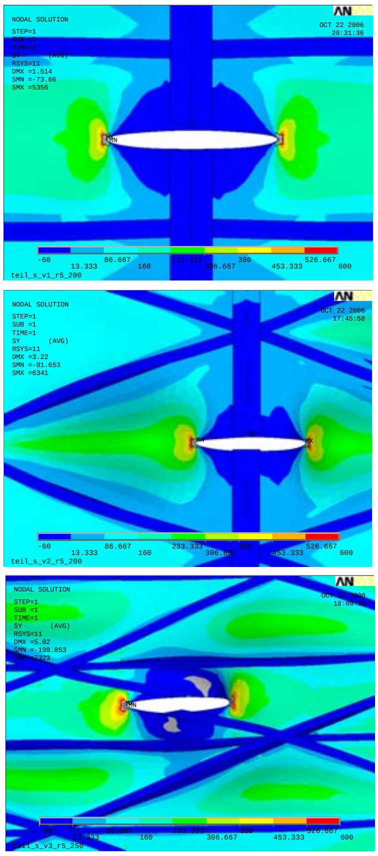

FIG. 5-7: Circumferential stresses for longitudinal two bay cracks, concepts “V1”, “V2” and “V3”

A two bay crack probably destroys the whole stiffener between these bays of an integrally stiffened structure. Such a damage may result from a welding defect. The scenario is shown in FIG. 5-7. The circumferential stresses are shown for a crack length of $2a$ = 200 mm. The associated stress intensities of Mode I are shown in FIG. 5-8. Similar to the one bay crack, concept “V3” results in the highest stress intensities. For small crack intensities, they exceed the stress intensities of “V1” and “V2” by 30 %, for long cracks even by 80 %. Comparing concepts “V1” to “V2”, “V1” is less critical for small crack lengths since the crossing axial stiffeners are closer to the crack than the tilted stiffeners in “V2”. The maximum is however reached earlier in “V2” due to the stiffening triangular bay. As the maximum level is below the maximum of “V1”, there is a positive effect in concept “V2”.

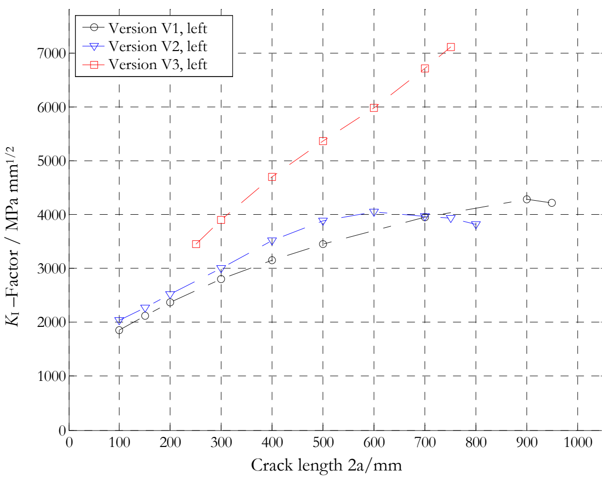

FIG. 5-8: K_I in a central longitudinal two bay crack; “V1”, “V2” and “V3”

5.3.3. Transition from one bay to two bay crack

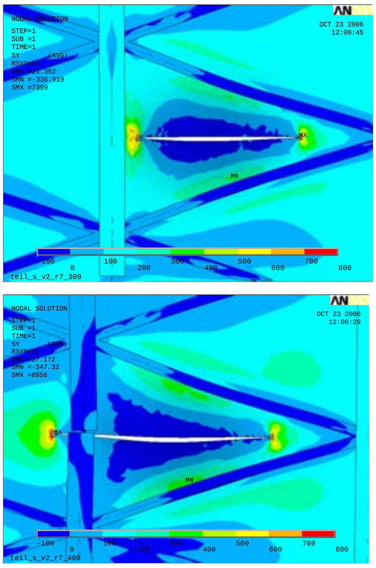

FIG. 5-9: Rupture of a stiffener in concept “V2”

In previous sections a crack prolongation was ascribed to both crack tips uniformly. This section deals with a one side prolongation. The right crack tip was fixed at a distance of 350 mm from the centre of the stiffener. The left crack tip position was varied to investigate three one bay crack scenarios and two two bay cracks with a broken stiffener (FIG. 5-9). The stress intensity (Mode I) is shown in FIG. 5-10. The dotted vertical line indicates the crack length at which the stiffener is reached. The first region generally represents the behaviour described in 5.3.1. A following separation of the stiffener leads to a sudden increase in concept “V1” caused by the loss of a load path and a resulting load redistribution. There is an impact of the two diverging stiffener parts on the crack tip. Afterwards the broken stiffener stabilises the crack since a further crack tip opening is stopped preliminarily before the known behaviour of a two bay crack dominates.

Concept “V2” shows a similar reaction in the two bay crack region. A significant difference can be found for the transition from a one to a two bay crack. The stress intensity remains almost constant. One reason may be the fact that circumferential loads are partly transmitted by the tilted stiffener and a loss of the circumferential stiffener is less severe.

The third concept, “V3”, takes again an unfavourable course since both the one as well as the two bay crack have a high gradient.

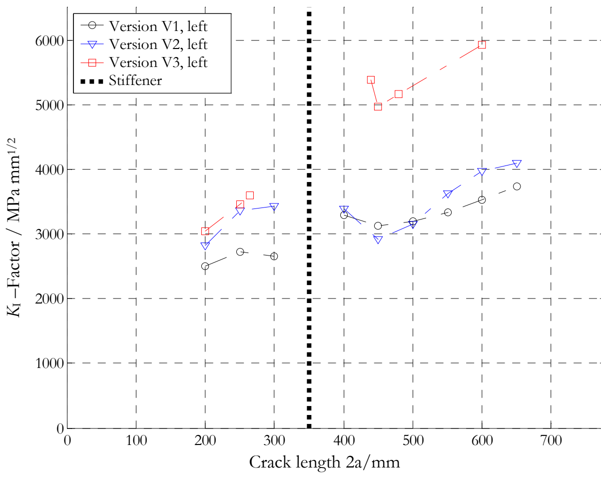

FIG. 5-10: K_I-Factor for a rupture of a stiffener for a growing longitudinal crack in concepts “V1”, “V2” and “V3”

5.3.4. Central circumferential one bay crack

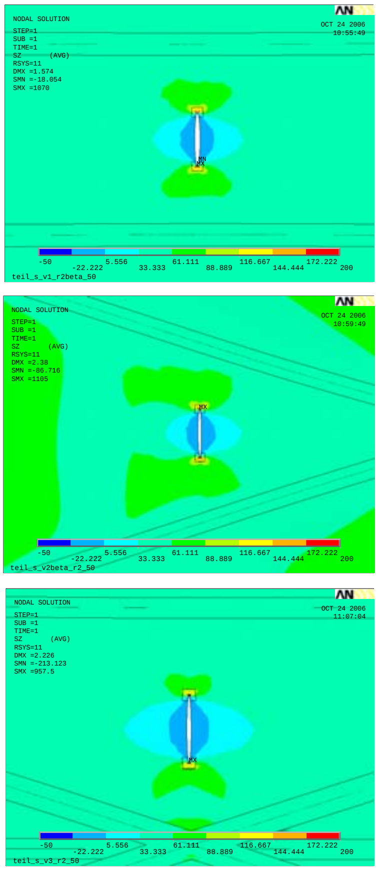

FIG. 5-11: Axial stresses for one bay cracks in circumferential orientation in “V1”, “V2” and “V3”

The second crack group is orientated circumferentially.

Similar to the longitudinal cracks, they were positioned centrally in the bay. The analysed crack length range was from $2a$ = 25 mm to 115 mm and 120 mm in “V3”. The range was again limited by the FE mesh generation. Referred to the distance of the stiffeners a relative crack length of 87 % (“V1”), 79 % (“V2”) and 78 % (“V3”) could be modelled.

The stress plots (FIG. 5-11) show the axial stresses, which is the perpendicular direction to the crack orientation, for a crack length of $2a$ = 50 mm.

Since concept “V2” has the lowest longitudinal stiffening, especially on the left side, the zone of higher stresses is extended into the less stiffened region of the field. Concept “V3” has the strongest longitudinal stiffening and therefore the lowest stress intensities. Both crack tips of “V3” have almost the same stress intensity; there is no significant positive influence of the stiffeners’ intersection because of their obtuse cutting angle.

Mode II and III are below 3% referred to the main Mode I, and therefore they are not discussed here.

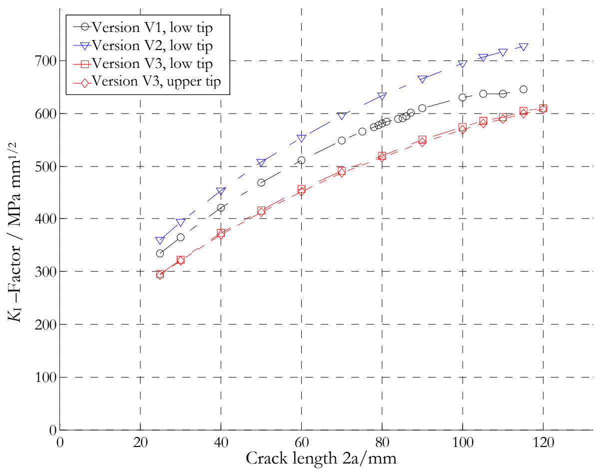

FIG. 5-12: K_I -Factor in a central circumferential one bay crack in concepts “V1”, “V2” and “V3”

5.3.5. Central circumferential two bay crack

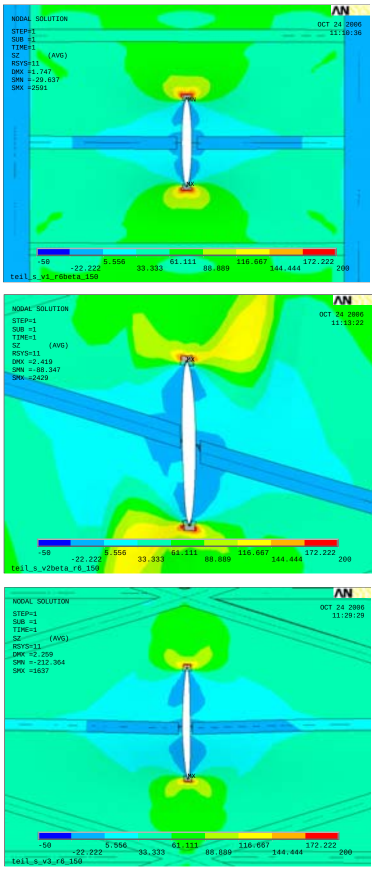

FIG. 5-13: Axial stresses for two bay cracks in circumferential orientation in “V1”, “V2” and “V3”

In case of a two bay crack, a length up to 86 % (“V1” & “V2”) and up to 89 % (“V3”) of the theoretical bay width could be realised. FIG. 5-13 shows the axial stresses for a crack of 150 mm length.
Concept “V2” leads to a point symmetric stress field. The stress indicates a high shear component within the crack tips.
Quantitatively, the stress intensity of Mode I (FIG. 5-14) indicates the same order of magnitude for the first two concepts. However, the intensity of “V3” is significantly lower than in “V2” and “V1”. The maximum is below 1000 MPa mm$^{1/2}$ which is 15 … 20 % lower than in concept “V1” or “V2”. Moreover, a stabilizing effect of the crossing areas is visible, as indicated by the plateau. This effect can be seen here, because the relative crack length could be increased (89 %) compared to the previously analysed one bay crack (78 %).
Further information can be yielded from Mode II and III (curves are not printed here). In concept “V1” and “V3”, these intensities are below 1 % but “V2” has maximum values of 14 % and 6 % in K_{II} and K_{III} respectively. The aspect of a significant K_{II}-Factor will be taken up in the next section.

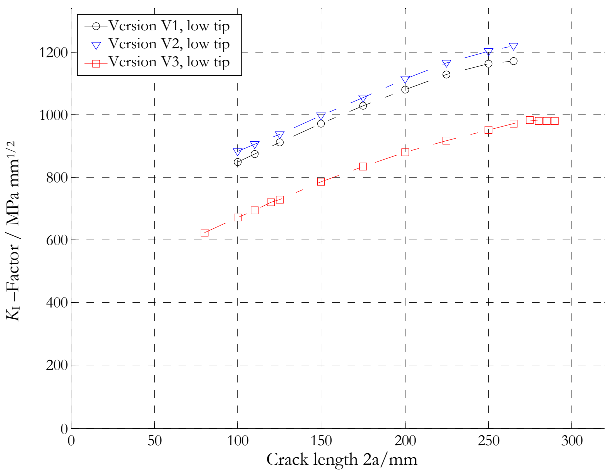

FIG. 5-14: K_I -Factor in a central circumferential two bay crack in concepts “V1”, “V2” and “V3”

5.3.6. Influence of crack deflection

The results have shown that a pure Mode I stress of the crack tip is not always given. According to 5.2. a non-linear crack propagation was implemented by incremental crack prolongation, taking into account the deflection angle φ_0. Both the longitudinal one bay crack in “V3” and the circumferential two bay crack in “V2” were analysed with crack deflection, since considerable Mode II stress was found (cf. sections 5.3.1 & 5.3.5). The following figures show the crack line in these two cases. The longitudinal crack reaches an offset referring to the original line of up to 10 mm for long cracks (FIG. 5-15). Remarkably, there is no strong progression in deflection when approaching the stiffeners, but a smooth deflection that already concerns cracks of 200 mm length (crack tip position +/- 100 mm).
The circumferential two bay crack in concept “V2” is deflected directly after the rupture of the tilted stiffener (FIG. 5-16). In the stress fields, this was already indicated by the high shear tendency.
Both non-linear curves yield a Mode I stress intensity very comparable to the already presented curve. Deviations in Mode I stress intensity amount to approx. 1 %. For this reason a further discussion of this deflection effect is not carried out here.

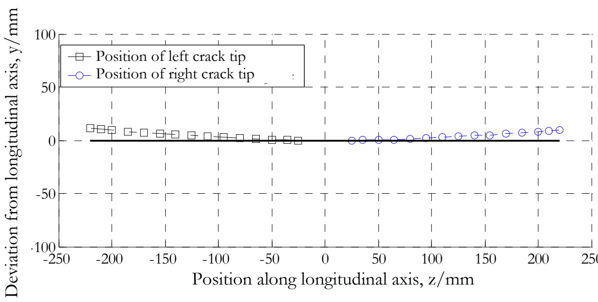

FIG: 5-15: Position of both crack tips referred to the horizontal line for a one bay longitudinal crack in concept “V3”

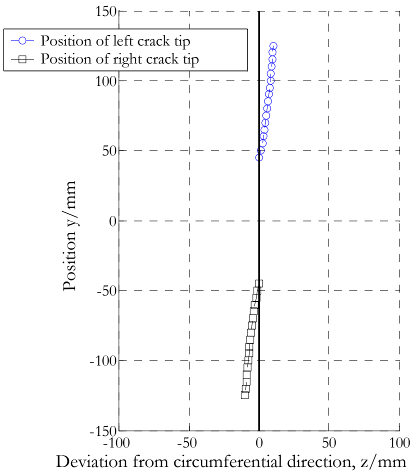

FIG. 5-16: Position of both crack tips referred to the circumferential line for a two bay circumferential crack in concept “V2”

5.3.7. Combined shear-tension loading

Additional attention was paid to a comparison of concepts “V1” and “V2” under combined shear-tension loading. Concept “V3” was not of interest due to preliminary investigations at the IFL, which are not object of this article.

According to the loading, described in 4.5.3., Mode I and II stress intensities are given in FIG. 5.17 and 5.18. Since the variation of the shear-tension ratio was performed through the change of tension, Mode I increases significantly, while Mode II principally remains on the same level. The K_I-Factor in the tilted stiffened "V2" is generally higher than in the rectangular "V1". Moreover, an increase of tensile stress causes a higher rise in K_I in concept "V2" than in "V1". A general disadvantage of "V2" compared to "V1" can be set to approximately 5%.

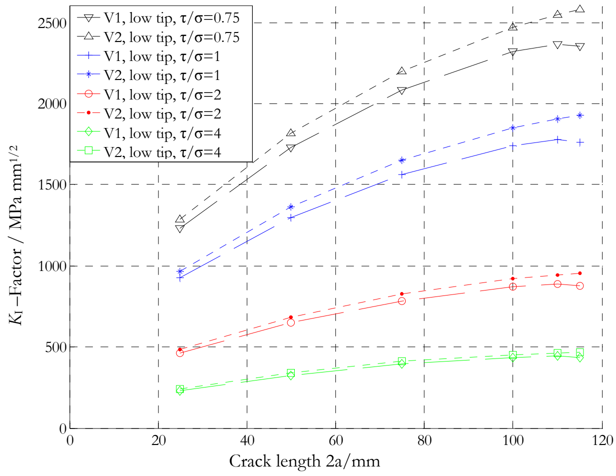

FIG. 5-17: K_I-Factor for circumferential one bay cracks under combined shear-tension loading, concepts "V1" and "V2"

The K_{II}-Factor does not change significantly for the different load ratios since the applied shear load is not varied between the load ratios. The rectangular concept "V1" is even completely independent since an increase in tensile fraction is not coupled with shear events in the bay. Concerning the tilted stiffened "V2", there is a dependency as tension and shear are coupled via tilted stiffeners. With regard to this second fracture mode, "V2" causes an approximately 10 % lower stress intensity. Slight differences between the upper and lower crack tip may be due to the different orientation of the tilted stiffener. While the crack would be turned to grow parallel to the stiffener on one side, it would grow perpendicularly to the stiffener on the other side regarding the same shear loading.

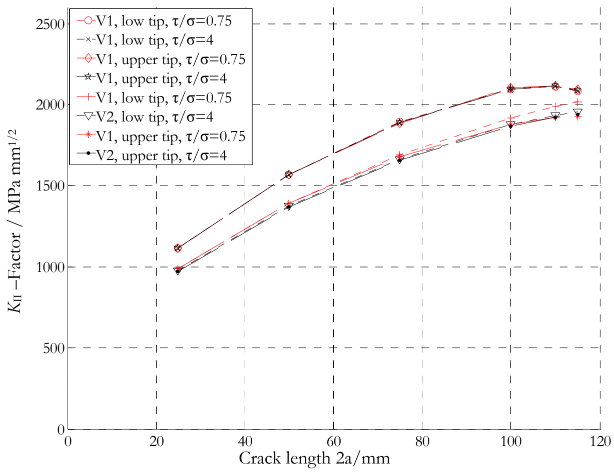

FIG. 5-18: K_{II}-Factor for circumferential one bay cracks under combined shear-tension loading, concepts "V1" and "V2"

6. CONCLUSION AND PERSPECTIVE

In the analyses, different stiffening concepts were analysed with regard to their influence on the stress intensities of selected crack and load scenarios. Although the variety of results makes it difficult to set clear benchmarks for the concepts, tendencies can be formulated for the exemplarily analysed cases.
Based on the classical rectangular concept, "V3" with its high longitudinal stiffening ratio is only useful under clear longitudinal tensile loading when dealing with circumferential cracks. However, the application is generally questionable since the concept shows a marked weakness concerning longitudinal cracks with their nearly linear increase in stress intensity.
Comparing concept "V1" to "V2", the criticality of longitudinal cracks is effectively reduced by the combination of the frame and the tilted stiffener on one crack side in "V2". However, this is accompanied by disadvantages at the second crack tip. It may be checked whether this behaviour can be used to define limited zones of higher crack criticality, e.g. for inspection. Moreover, a transition from a one bay to a two bay crack shows a preferable behaviour in concept "V2", since the stress intensity does not increase discontinuously with the loss of the circumferential stiffener. Circumferential cracks in the one bay scenario have a higher criticality in "V2" than in "V1", but this disadvantage is considerably reduced in the case of a two bay crack. Moreover, some potential could be located for shear-tension combination in "V2", whereby the tension loading should be dominant.
Further investigations should concentrate on concept "V2", especially in order to detect further advantages under combined shear loading, which is – depending on the location within the fuselage – present. Moreover, it could be analysed in how far a combination of different concepts in a fuselage might be reasonable to face the dominating load case in each region.

ACKNOWLEDGEMENT

The author would like to thank Prof. Dr.-Ing. P. Horst and Dipl.-Ing. A. Kiehne sincerely for their support and mentoring during and after the author's diploma thesis which served as a basis for this paper.

REFERENCES

[1] Blumenauer, H.; Pusch, G.: "Technische Bruchmechanik", 1. Auflage, VEB Deutscher Verlag für Grundstoffindustrie, Leipzig 1982
[2] ANSYS 10.0 Documentation
[3] Gross, D.; Seelig, Th.: "Bruchmechanik - mit einer Einführung in die Mikromechanik", 3. Auflage, Springer Verlag Berlin Heidelberg New York, 2001
[4] Paris, P. C.; and Sih, G. C.: "Stress Analysis of Cracks", Fracture Toughness and Testing and its Applications, American Society for Testing and Materials, Philadelphia, STP 381, pp. 30 - 83, 1965
[5] Horst, P.: "Umdruck zur Vorlesung Finite Elemente Methoden I (Leichtbau II) ", Institut für Flugzeugbau und Leichtbau, TU Braunschweig, Sommersemester 2004
[6] Horst, P.: "Damage Tolerance und Structural Reliability", Institut für Flugzeugbau und Leichtbau, TU Braunschweig, Sommersemester 2006
[7] Richard, H.-A.: "Bruchvorhersage bei überlagerter Normal- und Schubbeanspruchung von Rissen", VDI Forschungsheft 631, 1985
[8] PATRAN 2005 Documentation / PCL Manuals
[9] Zehnder, Alan T.: "Fracture Mechanics of Thin Plates and Shells Under Combined Membrane, Bending, and Twisting", Applied Mechanics Reviews, Vol. 58, No. 1, pp. 37 – 48, January 2005
[10] Pettit, R.G.; Wang, J. J.; C. Toh,: "Validated Feasibility Study of Integrally Stiffened Metallic Fuselage Panels for Reducing Manufacturing Costs", NASA/CR-2000-209342, May 2000
[11] Zhengtao, C.; Duo, W.: "A NEW FRACTURE CRITERION FOR MIXED MODE CRACK PROBLEM", International Journal of Fracture 64, R29 – R34, 1993
[12] Barsoum, I. S. "Mixed Mode Ductile Fracture – a literature review" September 2003, http://www.hallf.kth.se/~imad/imad_lit_study.pdf, Access on 30/10/2006